Supplementary Figure Legends

Supplementary Figure 1. Tumor growth. After cell injection, tumor kept growing in control group, while for mice received treatment, tumor started to shrink, scared over time and disappeared eventually.

Supplementary Figure 2. Shotgun proteomics identification and quantification of serum glycosylated proteins. (A) The efficiency of N-glycosylated peptides capture. X axis represents the sample number. (B) The percentage of glycoproteins for each sample. (C) The assignment of 8-plex iTRAQ reagent. Each sample was labeled with 8-plex iTRAQ reagent and mixed into Group A, B and C based on the treatment and time points. N, C, T represents healthy, untreated and treated mice, respectively. Numbers represent time points (2h, 2, 5, 8, 11, 14, 21, 28 days after treatment). After fractionation, each fraction was analyzed by LC-MS/MS and two technical replicates were required. (D) Proteins identification and quantification in each two replicates.

Supplementary Figure 3. (A) The cellular location of identified proteins. (B) The distribution of protein ratios within each time point. Each protein's intensity was compared with its partner in control group. The ratios were transformed to $\log_2$ value and fit the normal distribution. Thus, proteins' ratios outside the range of mean ± 2σ were considered as the significant proteins.

Supplementary Figure 4. The significantly enriched signaling pathways by IPA analysis. (A) The activated acute phase response 2 days after therapy. (B) The inhibited acute phase response 21~28 days post therapy. All of the colored proteins

represent those identified in our experiments and proteins in red are significantly up-regulated, while those in green are significantly down-regulated in mice treated.

Supplementary Figure 5. Quality assessment of instrument and peptide variation of mice serum. One peptide of angiotensin was spiked in each sample to assess the quality of instrument running. For each time point (N, C, T), most of the intra-mice CV value of angiotensin was below 20% and the CV value among different mice sample was 22%. Note: the error bars in red represent that the CV was more than 20% for this data set (29.48%, 22.90% and 31.04%). Data are shown as mean ± SD. n=5~6 for each sample set, expect that on 28^{th} day, only 3 mice survived in control group.

Supplementary Figure 6. Time course verification of significant proteins using parallel reaction monitoring. Significant proteins associated with (A) Acute phase response. (B) Tumor progression and metastasis. (C) Metabolism. Data are shown as mean ± SD. *$p < 0.05$, **$p < 0.01$, ***$p < 0.001$ by two-way ANOVA with the Bonferroni correction. n=5~6 for each condition, except that on 28^{th} day, only 3 mice survived in the control group.

Supplementary Figure 7. The protein expression profile of LIFR resulting from shotgun iTRAQ labeling quantification. Although there is no significant difference between mice treated and untreated, an apparent opposite trend could be obviously observed.

Supplementary Tables

Supplementary Table 1. 23 Target proteins with 32 precursors and corresponding 3~6 transitions used for quantification.

Supplementary Table 2. Linear regression of proteins' intensities of two technical replicates.

Supplementary Table 3. Proteins identified across three groups.

Supplementary Table 4. N-Glycoproteins quantified across all of the samples and their cellular location.

Supplementary Table 5. Significant glycoproteins quantified across the time course.

Supplementary Table 6. The information of peptides selected for PRM analysis and its significant expression profile quantified in iTRAQ labeling shotgun proteomics.

Supplementary Figure 1. Tumor growth.

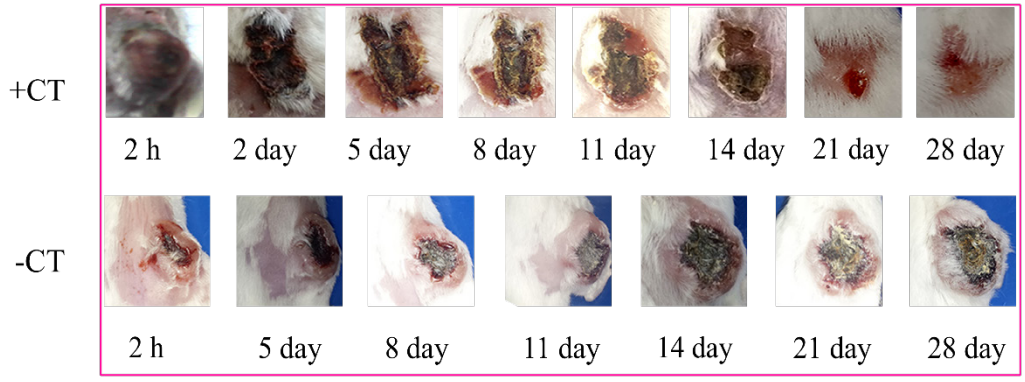

Supplementary Figure 2. Shotgun proteomics identification and quantification of serum glycosylated proteins.

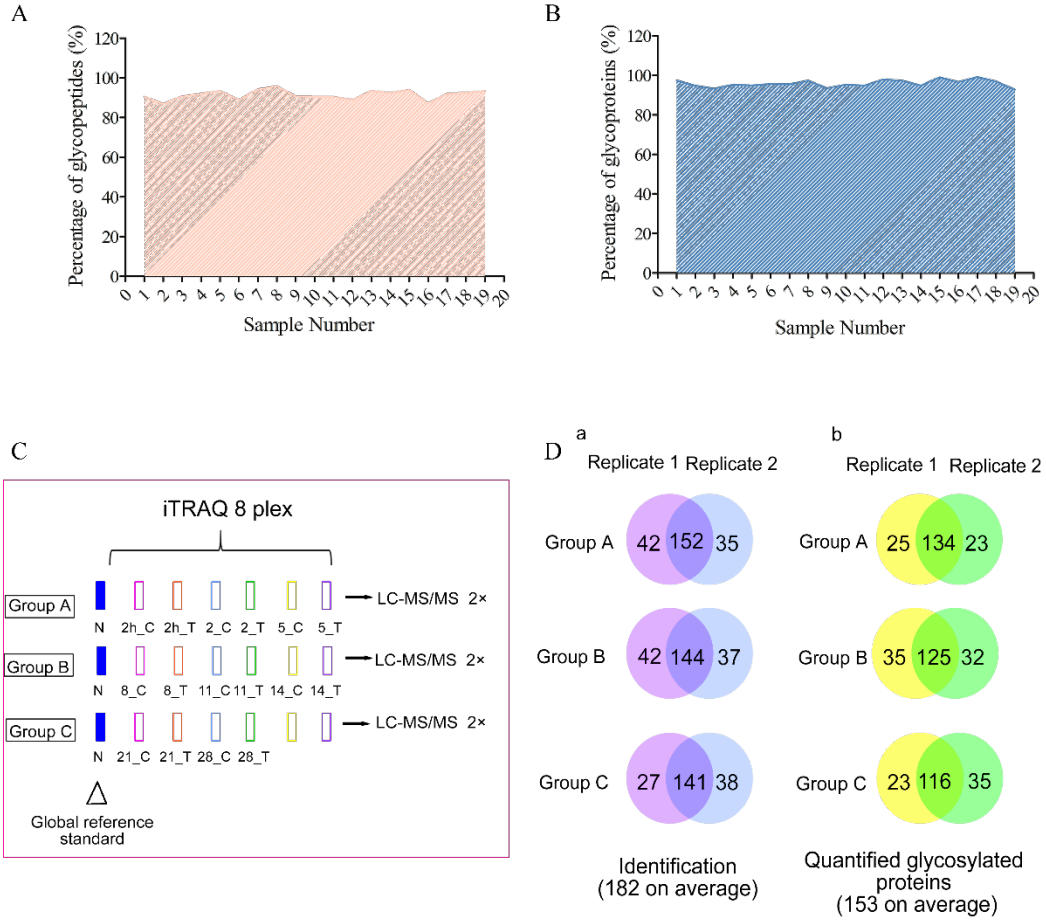

Supplementary Figure 3.

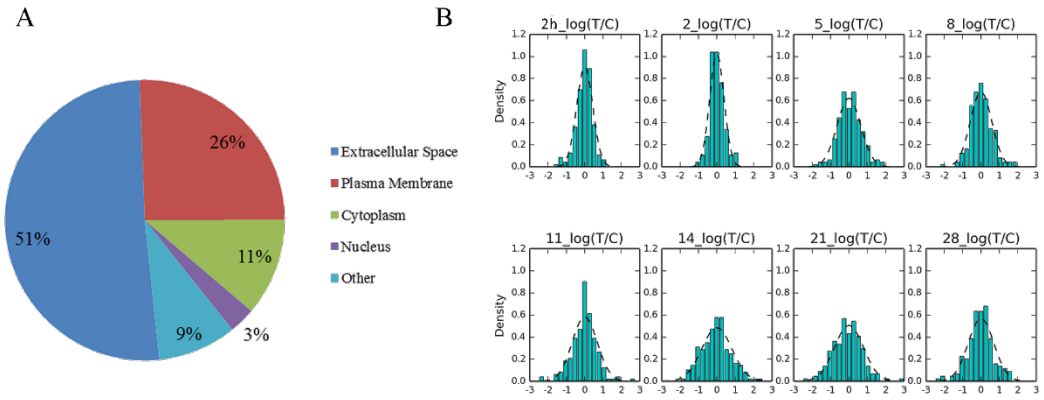

Supplementary Figure 4. The significantly enriched signaling pathways by IPA analysis.

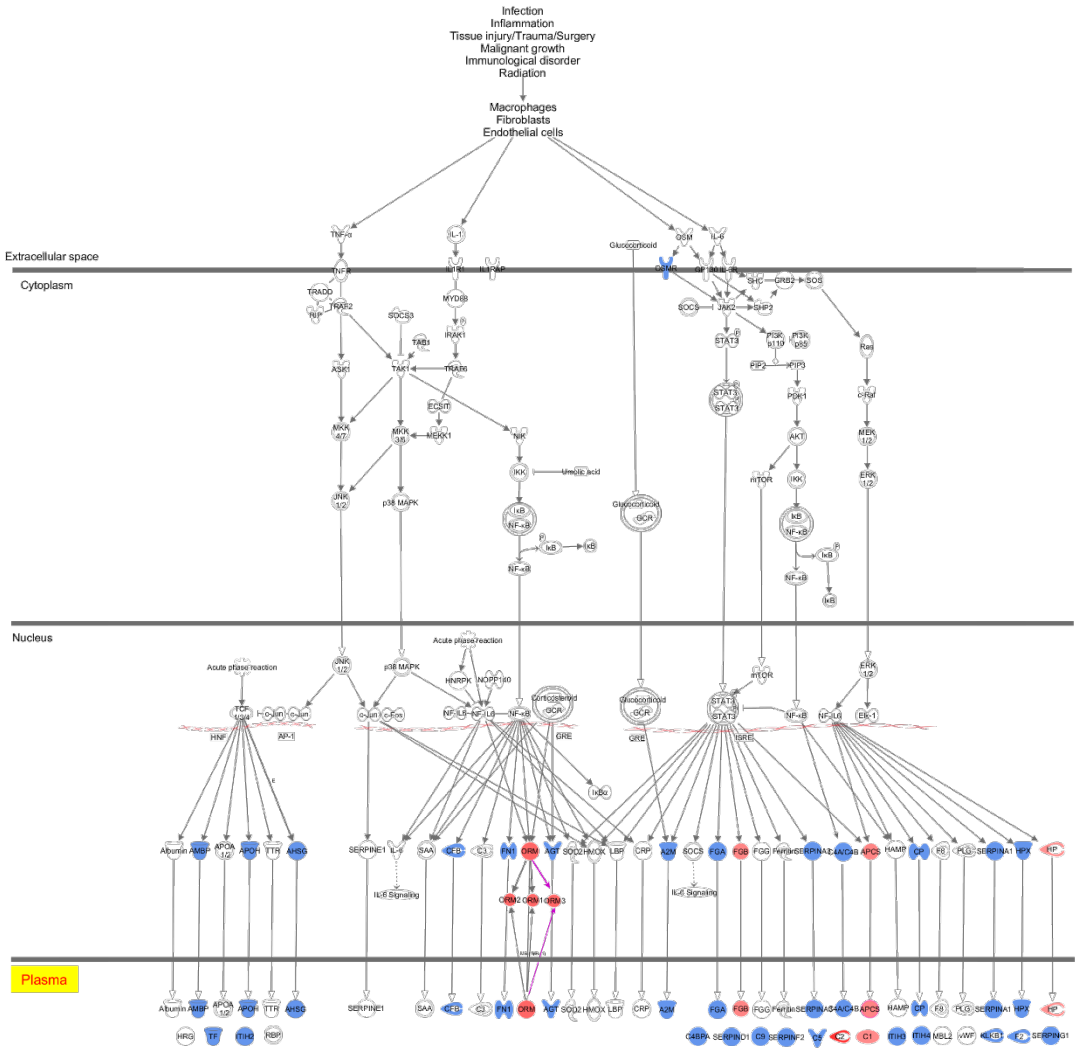

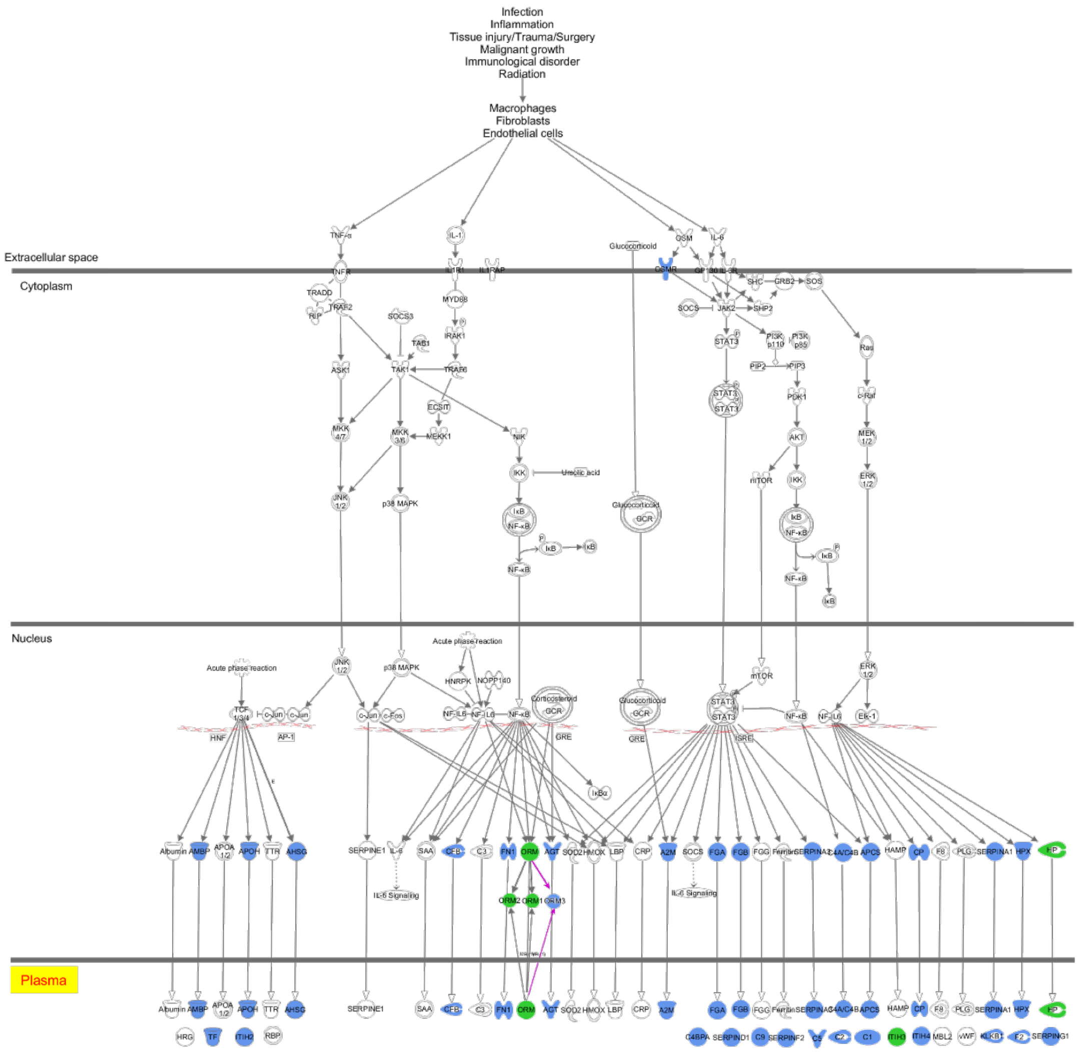
Infection
Inflammation
Tissue injury/Trauma/Surgery
Malignant growth
Immunological disorder
Radiation
Macrophages
Fibroblasts
Endothelial cells
Extracellular space
Cytoplasm
Nucleus
Plasma
TNF-α
IL-1
Glucocorticoid
OSM
IL-6
TRADD
RIP
TRAF2
SOCS3
MYD88
IRAK1
TAB1
ASK1
TAK1
TRAF6
ECSIT
MKK 4/7
MKK 3/6
MEKK1
NIK
IKK
JNK 1/2
p38 MAPK
IκB
NF-κB
SHC
GRB2
SOS
SOCS
JAK2
SHP2
STAT3
STAT1
PI3K
PIP2
PIP3
PDK1
AKT
mTOR
Ras
c-Raf
MEK 1/2
ERK 1/2
Acute phase reaction
HNRPK
c-Jun
c-Fos
AP-1
HNF
Corticosteroid
GCR
GRE
ISRE
Elk-1
IL-6 Signaling
Albumin
AMBP
APOA 1/2
APOH
TTR
AHSG
SERPINE1
SAA
CFB
C3
FN1
ORM
AGT
SOD2
HMOX
LBP
CRP
A2M
FGA
FGB
FGG
SERPINA3
C4A/C4B
APCS
HAMP
CP
F8
PLG
SERPINA1
HPX
HP
ORM2
ORM1
HRG
TF
ITIH2
RBP
C4BPA
SERPIND1
C9
SERPINF2
C5
C2
C1
ITIH3
ITIH4
MBL2
vWF
F2
SERPING1

Supplementary Figure 5. Quality assessment of instrument and peptide variation of mice serum.

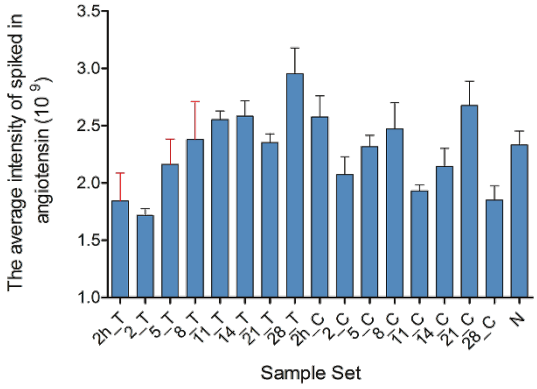

Supplementary Figure 6. Time course verification of significant proteins using parallel reaction monitoring.

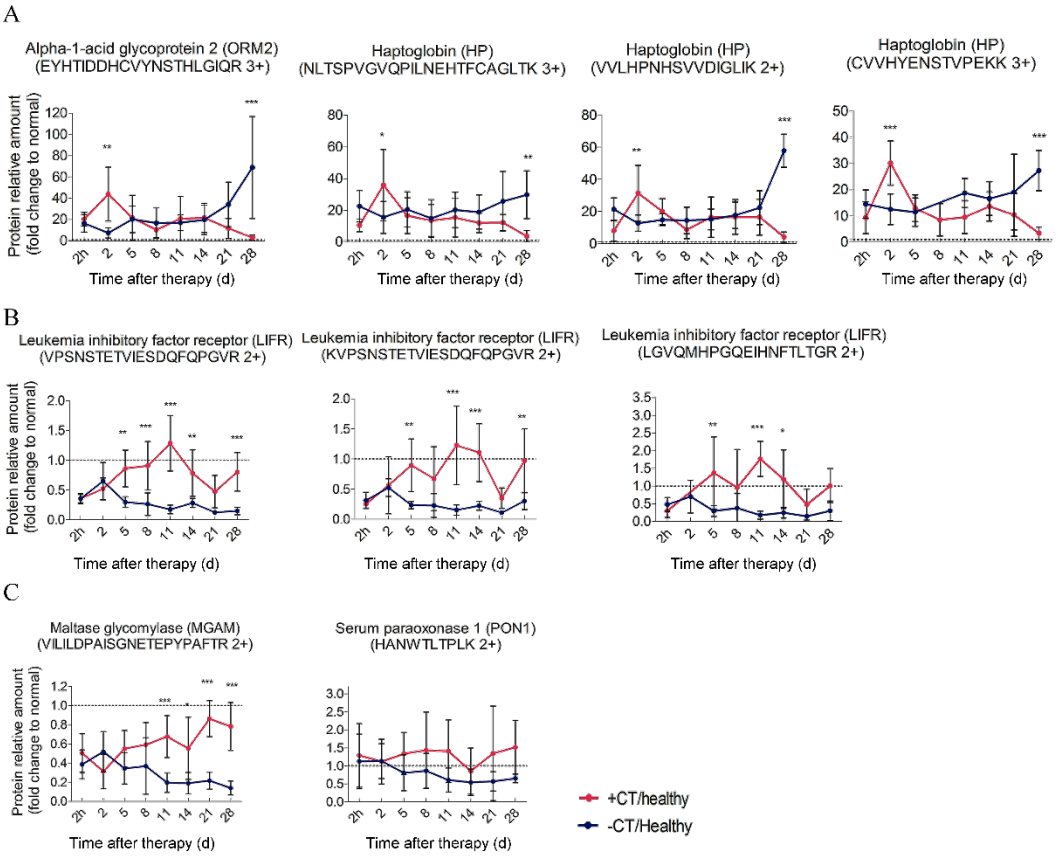

Supplementary Figure 7. The protein expression profile of LIFR resulting from shotgun iTRAQ labeling quantification.

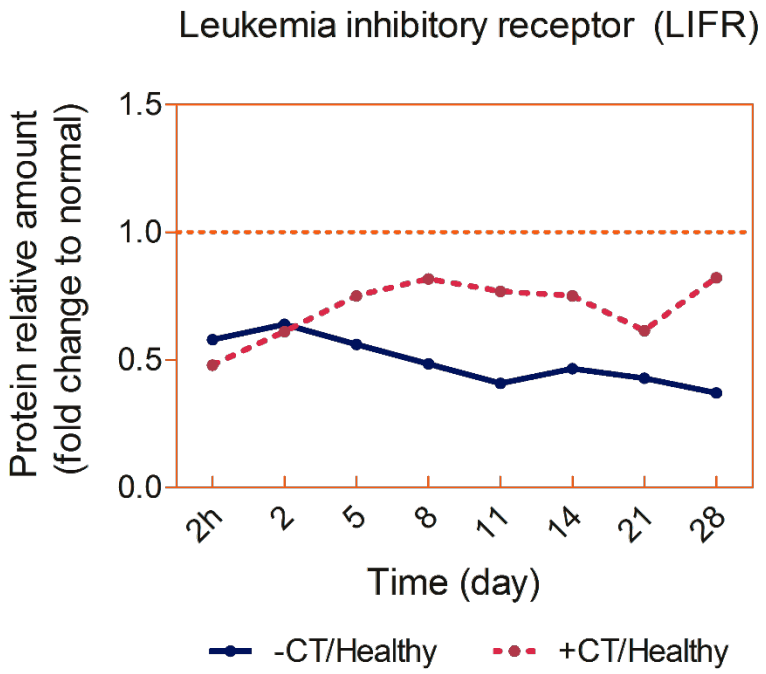

Graphical abstract

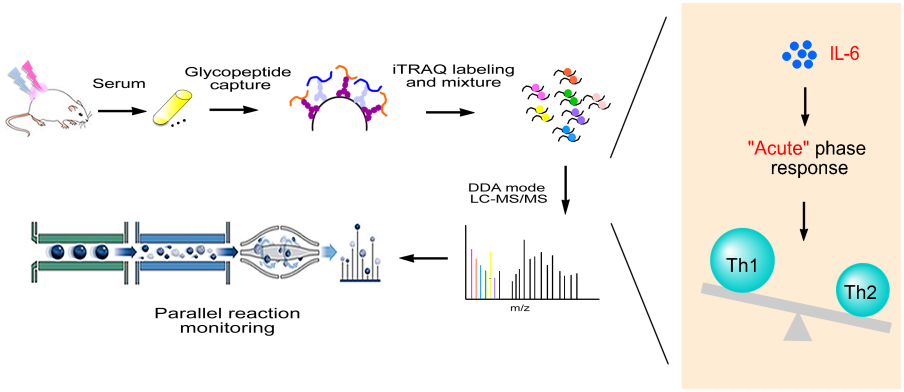

Serum glycoproteome using shotgun proteomics and parallel reaction monitoring technology revealed that interleukin-6 induced “acute” environment switched tumor microenvironment from Th2 immunosuppressive to Th1 immunostimulatory state after cryo-thermal therapy.